



HAL
open science

Molecular ordering dependent charge transport in π -stacked triphenylene based discotic liquid crystals and its correlation with dielectric properties

Asmita Shah, Dharmendra Pratap Singh, Benoit Duponchel, Freddy Krasisnski, Abdelylah Daoudi, Sandeep Kumar, Redouane Douali

► To cite this version:

Asmita Shah, Dharmendra Pratap Singh, Benoit Duponchel, Freddy Krasisnski, Abdelylah Daoudi, et al.. Molecular ordering dependent charge transport in π -stacked triphenylene based discotic liquid crystals and its correlation with dielectric properties. *Journal of Molecular Liquids*, 2021, 342, pp.117353. 10.1016/j.molliq.2021.117353 . hal-04456880

HAL Id: hal-04456880

<https://ulco.hal.science/hal-04456880v1>

Submitted on 22 Jul 2024

HAL is a multi-disciplinary open access archive for the deposit and dissemination of scientific research documents, whether they are published or not. The documents may come from teaching and research institutions in France or abroad, or from public or private research centers.

L'archive ouverte pluridisciplinaire **HAL**, est destinée au dépôt et à la diffusion de documents scientifiques de niveau recherche, publiés ou non, émanant des établissements d'enseignement et de recherche français ou étrangers, des laboratoires publics ou privés.



Distributed under a Creative Commons Attribution - NonCommercial 4.0 International License

Molecular ordering dependent charge transport in π -stacked triphenylene based discotic liquid crystals and its correlation with dielectric properties

Asmita Shah^{a,*}, Dharmendra Pratap Singh^a, Benoit Duponchel^b, Freddy Krasinski^a, Abdelylah Daoudi^b, Sandeep Kumar^{c,d} and Redouane Douali^a

^aUniv. Littoral Côte d'Opale, UR 4476, UDSMM, Unité de Dynamique et Structure des Matériaux Moléculaires, F-62228 Calais, France

^bUniv. Littoral Côte d'Opale, UR 4476, UDSMM, Unité de Dynamique et Structure des Matériaux Moléculaires, F-59140 Dunkerque, France

^cRaman Research Institute, Bangalore, 560080-India

^dDepartment of Chemistry, Nitte Meenakshi Institute of Technology (NMIT), Yelahanka, Bangalore, India

ARTICLE INFO

Keywords:

Discotic liquid crystal
Charge transport
Hole mobility
Dielectric property

ABSTRACT

We investigate the charge transport in triphenylene core based homologous series of discotic mesogens (HAT_n) by the time-of-flight method. HAT5, HAT6 and HAT8 exhibit Col_n phase whereas HAT4 shows Col_{hp} phase. For the investigated homologous series, we have observed a single transit in the transient photocurrent curves corresponding to positive charge carriers having the mobility in order of 10⁻² to 10⁻⁴ cm²/Vs. The hole mobility decreases with increasing the number of carbon atoms (*n*) in the alkyl chain attached to the triphenylene core, which follows the empirical exponential relationship: $\mu \approx a.exp(-b/n)$. Furthermore, the dielectric measurement has been done on these compounds to bring a correlation between the molecular ordering by varying the alkyl chain of the HAT_n compounds. In the light of structure-property correlation, we have noticed that the hole mobility and permittivity vary according to the length of alkyl chain attached to the triphenylene core. The molecular ordering is also discussed via phase behaviour of compounds and confirmed by polarized optical textures. The change in entropy also decreases with increasing alkyl chain length of the HAT_n compounds rendering an agreement with that of the mobility and dielectric measurements. The HAT_n compounds show their potential applications in opto-electronics and could serve as organic semiconductors; however, the poor conductivity remains as a futuristic challenge.

1. Introduction

Discotic liquid crystals (DLCs), abbreviated due to their disk-like shape of molecules, belong to a particular family of liquid crystals that are acquiring a great interest of researchers due to their specific use in organic semiconductor devices [1]. The ordering in DLCs is important to evaluate the performance of these semiconductor devices. Furthermore, molecular dynamics is crucial in recovering with structural defects. Owing to the π -conjugated structural superiority, DLCs include the order and dynamics together that offers a decisive advantage of controlling the physical properties of semiconductor devices [2, 3].


The molecular geometry of DLCs is constituted by the rigid poly-aromatic π -conjugated cores and peripheral flexible alkyl chains fastened via particular linking groups such as benzoate, ester, ether, etc. The stacking of discotic mesogens into 1D columns is a leitmotif in the self-organization of DLCs with a 2D crystalline structure with the plane perpendicular to the columns. The π - π stacking leads to a commonly observed hexagonal or rectangular columnar (Col_h or Col_r) phases [4, 5, 6], with a core-core separation about 3.5 Å and an intercolumnar distance of the order of 20–40 Å depending on the nature and the length of alkyl chains


[7, 8]. The formation of such phases eventuate due to the existence of supramolecular interactions like van der Waals forces, hydrogen bonding, charge-transfer interactions, etc [9, 10]. The molecular arrangement of DLCs makes them advantageous over the calamitic LCs for applications in electronic devices due to their larger overlapping of the molecular orbitals and their correlation of 1D charge transport and ability to tailor the emissive properties by controlling the mutual orientation of transition dipoles via disc rotations [11].

The π -conjugated aromatic core systems of DLCs make them ample in the charge transport which is often perceived via hopping mechanism. The charge transport properties significantly depend upon the electron-rich/deficient nature of the core and the molecular ordering. The charge transport properties have been advantageous and crucial for the performance of organic electronics. On behalf of 1D charge and energy transport, discotic mesogens play a toolbox in the evolution of sundry optoelectronic applications such as xerographic copiers [12], laser printers [3], organic photovoltaic solar cells [13, 14, 15, 8], organic light-emitting diodes (OLEDs) [16, 17, 11], organic field-effect transistors (OFETs) [18], liquid crystal displays [19], holographic optical data storage devices [20, 21], gas sensors [22], etc.

The hexaalkoxytriphenylene discotic mesogens have been extensively studied as organic semiconductors [23]. The different homologous, usually abbreviated as HAT_n (where *n* corresponds to number of carbon atoms in the alkyl chain: C_nH_{2n+1}, *n* = 4 to 13), exhibit a wide columnar mesophase

*Corresponding author

 asmita.shah@etu.univ-littoral.fr (A. Shah)

 <https://udsmm.univ-littoral.fr/> (A. Shah)

ORCID(s):

regime above the room temperature and show thermal and chemical stability during the heating and cooling cycles [24, 25]. Besides experimental analysis, various models have been outlined to explain the charge transport mechanisms in HAT_n DLCs. Palenberg *et al.* [26] have proposed a theoretical description of the dynamic disorder model for the temperature dependence of charge carrier mobilities of the electrons and holes by proposing the concept of stochastic Haken-Strobl-Reineker model. Later on, Kreouzis *et al.* [27] have incorporated the Holstein small polaron model to explain the temperature independent hole mobility in the binary discotic mixtures of the HAT6:PTP9 and HAT11:PTP9. Following to this study, Duzhko *et al.* [28] have also accounted the polaron model on the HAT5 DLC and disclosed that the decreasing mobility of charge carriers with increasing temperature is consistent with the Holstein small polaron theory in the nonadiabatic limit below the Debye temperature.

In the present article, the charge transport mechanism including the determination of hole mobilities of the hexaalkoxytriphenylene discotic mesogens (HAT_n) has been collectively re-investigated in spite of numerous studies done by parts in the past. Dielectric measurements have also been carried out for the HAT_n compounds to establish the variation of dielectric permittivity with increasing temperature and alkyl chain length of the HAT_n ($n = 4, 5, 6$ and 8) homologous. Henceforth, some properties of these DLCs deserve to be clarified. As an example, the phase behaviour of the HAT4 includes contradictory information on the existence of the columnar plastic and crystalline intermediate phase. In addition to the above consequences, a correlation between the maximum charge carrier mobility and permittivity in terms of molecular ordering is presented as the main theme of the article. The experimental findings via ToF and dielectric measurements have been further supported by the polarized optical microscopy and change in entropy.

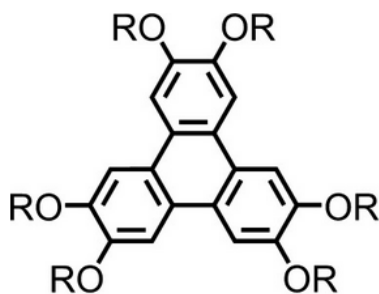


Figure 1: The chemical structure of hexaalkoxytriphenylene (HAT_n) discotic liquid crystal with $R = C_nH_{2n+1}$.

2. Materials and experimental details

The general chemical structure of hexaalkoxytriphenylene DLCs is shown in Figure 1. The members of the homologous series of HAT_n were synthesized as per standard protocol reported by Kumar *et al.* [29]. Herein, four mem-

bers (namely HAT4, HAT5, HAT6 and HAT8) of the HAT_n series have been taken for the investigation. Phase transition temperatures and the associated enthalpies were determined by utilizing TA Instruments Q1000 Differential Scanning Calorimeter with a ± 5 °C/min heating and cooling rates. UV-visible absorption measurements were carried out using Agilent Varian Cary 100 with a standard 10 mm integrated quartz cuvette. Absorption spectra were taken in the range from 190 nm to 1000 nm in solution state. The concentration of the solution was 0.1 mg/mL, using chloroform as the solvent. The reference and the background scans were carefully filtered before executing the absorption measurements on the HAT_n compounds.

For polarized optical microscopy (POMs) studies, charge mobility measurements and dielectric characterization, commercially available AWAT (Poland) cells of thickness 9.2 μm were used. The cells are constituted by two ITO coated glasses having a polyimide layer that prefers homeotropic orientation. It has been reported in the previous articles that the HAT_n homologous compounds orient homeotropically (columns perpendicular to the glass substrate) without showing any significant influence on the alignment layer [30, 31]. The HAT_n compounds were capillary-filled in the isotropic phase and the sample was cooled with a slow rate of 0.01 °C/min. The POM study was performed by utilizing a Zesis AXIO polarized optical microscope equipped with Infinity-2 software. During the POM study, the temperature of the HAT_n compounds were maintained by a Linkam TMS 94 hotplate.

Charge mobility and dielectric measurements were performed by utilizing specific sub miniature version A (SMA) connectors allowing contact on ITO electrodes. The temperature was controlled by means of a custom-made temperature controller Eurotherm 3504 and equipped with a temperature sensor (resistor Pt100). The real ϵ' and imaginary ϵ'' parts of the complex dielectric permittivity were calculated from impedance measurements by means of an HP4284A LCR meter in the frequency range of 20 Hz-1 MHz. The charge carrier mobility measurement was performed by time-of-flight (TOF) technique [30, 32, 11, 33, 34]. The sample is excited by means of Nd:YAG laser ($\lambda = 355$ nm, pulse duration = 5 ns). The photo-generated carriers propagate between the top and the bottom electrodes under the application of applied voltage supplied by a Keithley 6487 voltage source. The photocurrent is recorded by utilizing a current shunt resistor with a voltage amplifier (Stanford Research Systems SR560) and a digital oscilloscope (Keysight InfiniVision DSOX3022T). The charge carrier mobility (μ) was estimated by using the following relation:

$$\mu = d^2 / V \tau_{tr} \quad (1)$$

where, V is the applied voltage, d is the thickness of the cell and τ_{tr} is the transit time of the charge carriers. τ_{tr} is determined from the inflection point of the transient photocurrent curve.

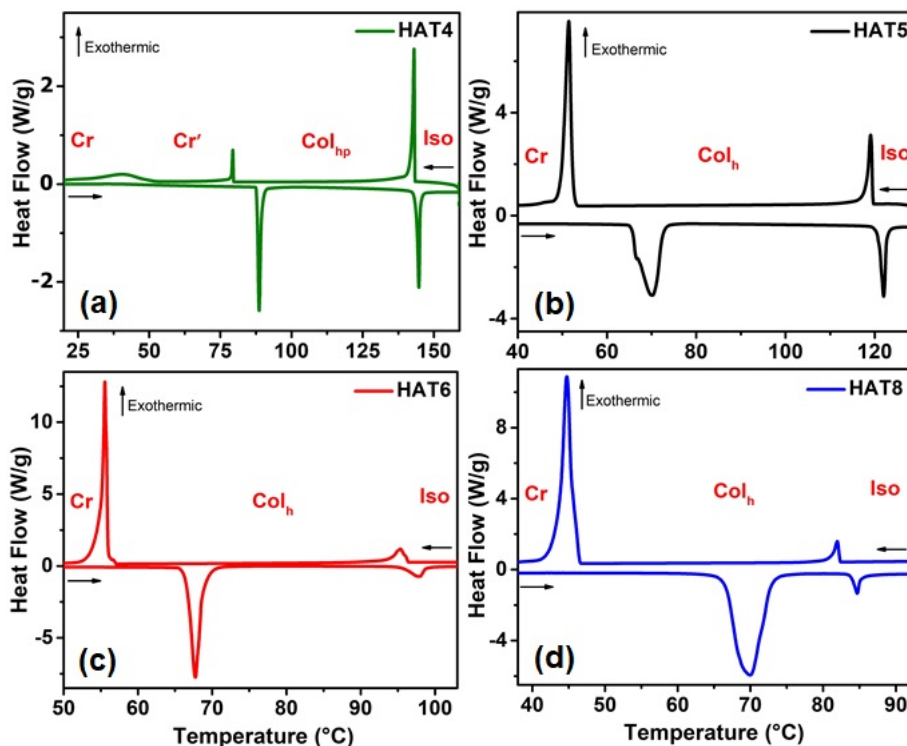


Figure 2: DSC thermograms of heating and cooling cycles of HAT4 (a), HAT5 (b), HAT6 (c) and HAT8 (d). Representation of the heating and cooling cycles is depicted by (→) and (←), respectively.

3. Results and discussion

3.1. Differential scanning calorimetric studies

The phase transition temperatures and their corresponding enthalpies of the HAT_n compounds were determined from the normalized differential scanning thermograms shown in Figure 2. Mesomorphic compounds exhibit a rationally low isotropic temperature (< 200 °C). During the cooling cycle, HAT4 shows columnar plastic (Col_{hp}) phase while HAT5, HAT6 and HAT8 render hexagonal columnar (Col_h) phase [35]. The greater ordering in the columnar plastic (Col_{hp}) phase is due to its three-dimensional crystal-like order (the discs within the columns are able to rotate about the columnar axis) whereas HAT5, HAT6 and HAT8 show a lower ordering in the hexagonal cloumnar (Col_h) phase due to its structural disorder-like lateral and longitudinal displacement of the discs and its nonparallel arrangement [36]. On cooling from the columnar phase, HAT4 exhibits two crystalline phases viz: Cr' and Cr while HAT5, HAT6 and HAT8 render single crystalline phase. The presence of the intermediate Cr' phase in HAT4 may be due to the compact structure of the compound that leads to the partial crystallization during the super cooling.

It is observed that the columnar–isotropic phase transition temperature decreases with increasing alkyl chain length in the HAT_n compounds, as the long alkyl chain induces the flexibility to the rigid core structure that leads to the decrease in the isotropic temperature [37]. From structural point of view, increasing chain length induces an increase in the molecular flexibility, fluctuations and disorder in the

the HAT_n compounds resulting in an increase in the inter-columnar distance [38]. This leads to decrease in the mesophase stability and hence in the transition temperature from isotropic to liquid crystalline phases [39]. Our results summarized in Table 1, agree well with this observation. It is evident from Table 1 that the enthalpy values, corresponding to isotropic-columnar and columnar-crystalline phase transition are gradually changed according to the alkyl chain length. Aforementioned thermal behaviour of HAT_n compounds is in good agreement with the reported literature [40].

3.2. Polarized optical microscopic studies

The optical textures of the HAT_n compounds were explored by using the polarized optical microscopy. The polarized optical micrographs (POMs), illustrated in Figure 3, show the classical birefringent textures of the HAT4, HAT5, HAT6 and HAT8 compounds. Figure 3 (a) depicts the mini mosaic texture for the columnar plastic phase of the HAT4 during the heating cycle. Whereas, Figures 3 (b) and (c) in cooling cycle, show the dendritic and mosaic patterns for the columnar plastic and crystalline intermediate phases, respectively. It is observed that the domain size of mosaic texture in cooling cycle is larger as compared to those observed in heating cycle. The difference in domain size has a cognation between the ordering of columnar phase and a uniform molecular orientation of the large number of columns. If the domain size of the mosaic texture is greater, it resembles the better alignment of the sample. Furthermore, Figures 3 (d), (g) and (j) show more polydomain textures of the HAT5, HAT6 and HAT8 during heating. Whereas, during cooling

Mesophase, transition temperature and enthalpy changes		
Compound	Cooling cycle	Heating cycle
HAT4	I 143.04 (107.60) Col _{hp} 79.37 (16.00) Cr' 41.10 (3.01) Cr	Cr 88.63 (108.10) Col _{hp} 144.74 (92.85) I
HAT5	I 119.10 (45.62) Col _h 51.48 (163.60) Cr	Cr 70.19 (148.40) Col _h 122.08 (39.94) I
HAT6	I 95.38 (20.94) Col _h 55.55 (173.60) Cr	Cr 67.74 (156.60) Col _h 97.95 (18.67) I
HAT8	I 81.94 (16.34) Col _h 44.80 (260.30) Cr	Cr 69.94 (223.00) Col _h 84.74 (14.22) I

Table 1

Phase transition temperatures (in °C) with the corresponding enthalpy changes (in J/g) observed upon heating and cooling with a rate of 5 °C/min; where I = Isotropic liquid phase, Col_h = Hexagonal columnar phase, Col_{hp} = Columnar plastic phase, Cr' = crystalline intermediate phase and Cr = crystalline phase.

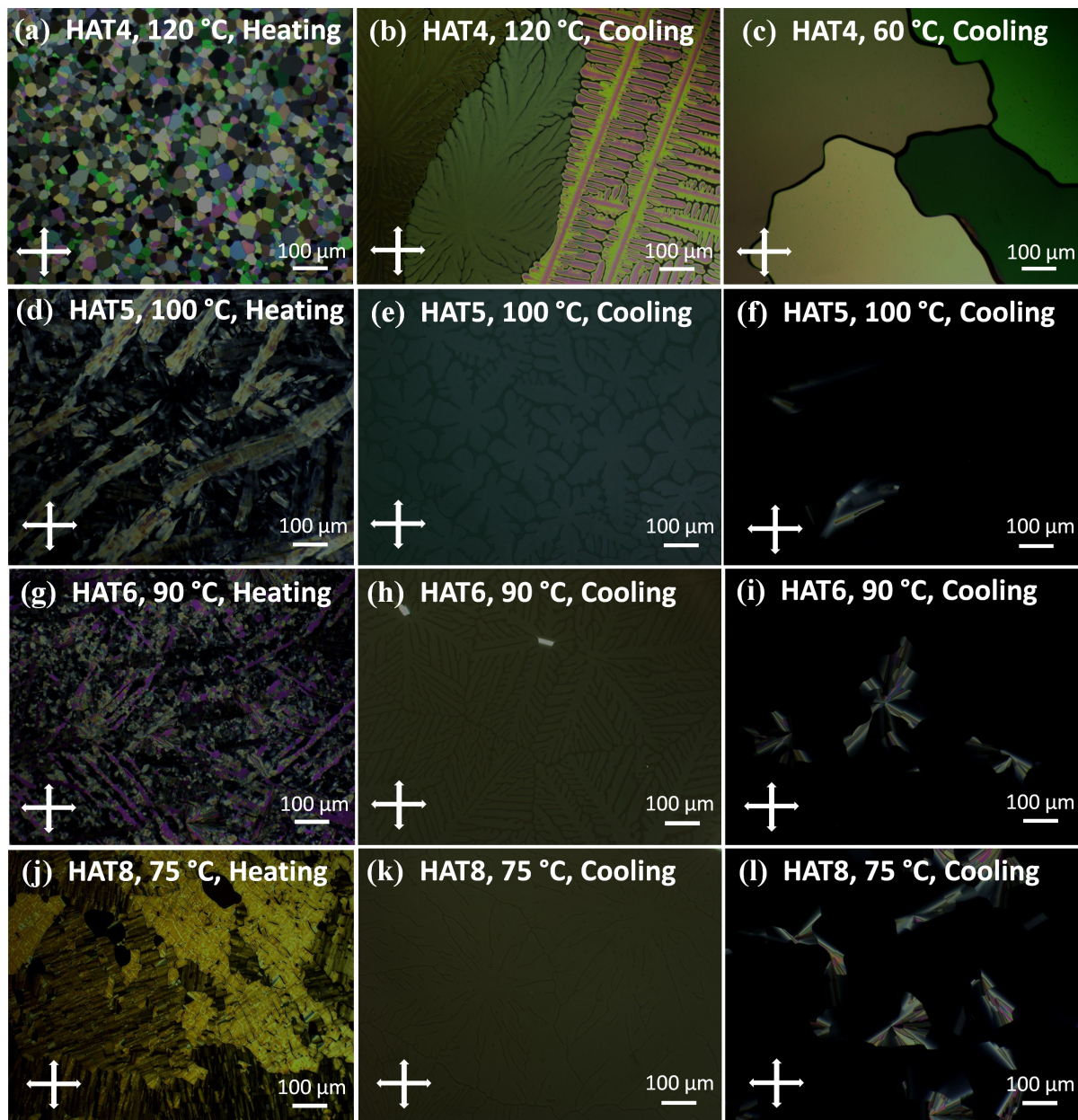


Figure 3: Polarized optical micrographs (POMs) in heating and cooling cycles of HAT4 (a, b and c), HAT5 (d, e and f), HAT6 (g, h and i) and HAT8 (j, k and m) respectively. The POM textures (e, h and k) was recorded under high light illumination whereas (f, i and l) was recorded under lower light illumination on another spot on the respective samples. The crossed arrows represent the crossed polarizer–analyzer condition. The cell thickness was 9.2 μm for all samples.

Figures 3 (e), (h) and (k) show the uniform and homogeneous classical dendritic textures of the DLCs [41]. The optical textures have vital importance in the identification of LC phase and the presence of defects or deformations. Under the crossed polarized condition, the textures of HAT5, HAT6 and HAT8 shown in figures 3 (f), (i) and (l) correspond to the homeotropic alignment with some defects and do not evince any birefringence due to uniform refractive index in all directions. The optic axis of homeotropically aligned discotic molecules coincides with column axis in columnar hexagonal phase. In figures 3 (f), (i) and (l), the textures appear black with few defects. With increasing alkyl chain the defects become more significant because of the disruption in the orientation of column leading to the reduction in the ordering of the HAT_n compounds [42].

3.3. Charge carrier mobility measurement

After studying the molecular ordering in the HAT_n compounds, its subsequent effect on the charge transport property has been investigated. The mobility of positive charge carriers (i.e. holes) in the HAT_n compounds was examined by the time-of-flight technique. In the ToF method, the HAT_n compounds were excited by a Nd:YAG pulsed laser with 355 nm excitation wavelength. HAT_n compounds are known to exhibit various absorption peaks between 280 to 360 nm; however, with the help of the UV-visible absorption spectra presented in Figure (4), we have demonstrated that HAT_n compounds absorb sufficient radiation of 355 nm and subsequently are able to liberate the charge carriers. The absorption spectrum provides in-depth information about the electronic transitions. The spectra of the HAT_n compounds show an absorption peak nearly at 350 nm attributed to π - π^* transitions in the C=C bonds of the triphenylene core [33]. In contrast to previously published articles [43, 44], we have observed a slight red-shift in the absorption peak for the HAT_n compounds that might be due to the change in solution concentration following to the Beer-Lambert law [45, 46]:

$$I = I_0(-c)^n \exp(\epsilon \cdot l) \quad (2)$$

where, I_0 and I are the intensities of the incident and transmitted radiations, respectively. c and l are the solution concentration and optical path length, respectively, and ϵ is the absorption coefficient. n is the power exponent. It is a well-known fact that the absorption character remarkably depends on the concentration and nature of the solvent. Subsequently, the absorption peak and magnitude of absorption can be altered by changing the concentration and nature of solvent. It is perceived that as the alkyl chain length attached to the triphenylene core increases, the absorption has been decreased. This decrease in absorption is probably due to the inductive effect of the stabilizing carbocation mechanism [47]. This reduces the contribution of electron on oxygen atom in the ring conjugation resulting into increased gap between the HOMO (highest occupied molecular orbital) and LUMO (lowest unoccupied molecular orbital).

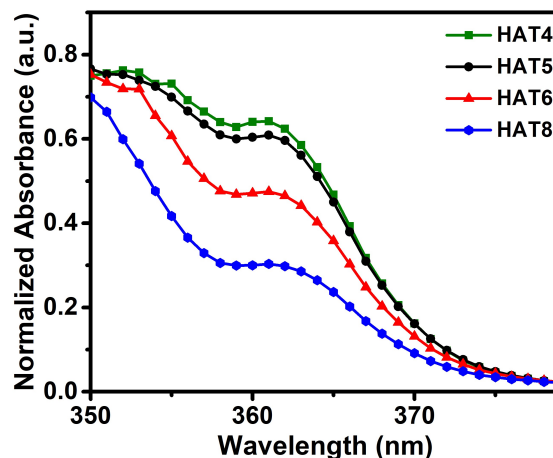


Figure 4: Normalized absorbance spectra of the HAT4, HAT5, HAT6 and HAT8. Chloroform has been taken as the solvent with the concentration of 0.1 mg/mL.

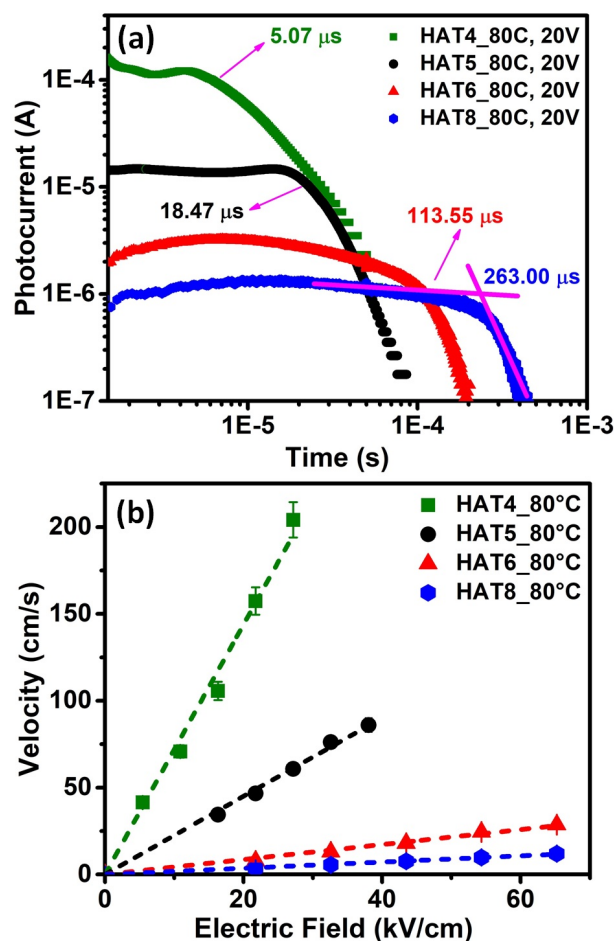


Figure 5: (a) Transient photocurrent curves measured by TOF technique from the double logarithmic plots of HAT4, HAT5, HAT6 and HAT8 with 9.2 μ m cell thickness at 80 °C in the columnar phase, (b) Drift velocity versus electric field curve was linearly fitted to obtain the value of hole mobility.

Charge carrier mobility measurements were carried out in the cooling cycle. Under the application of bias voltage,

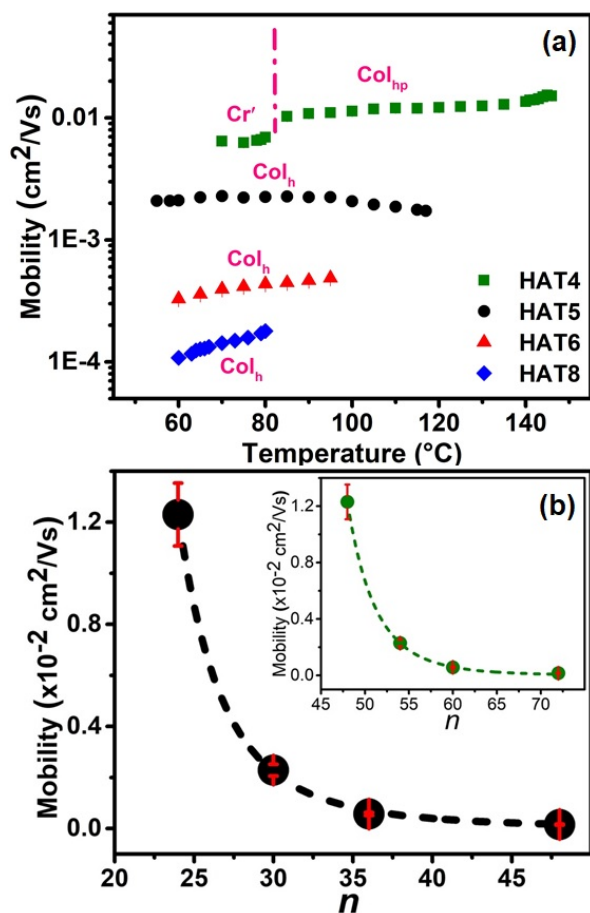


Figure 6: Mobility measurements by TOF technique for HAT4, HAT5, HAT6 and HAT8: (a) Temperature dependence of the charge carrier mobilities of holes, the error bars shows the maximum error of $\pm 3\%$ in the experimental data, (b) Alkyl chain length dependence hole mobilities, where n represents the number of C (carbon) atoms in the alkyl chain of HAT_{*n*} compounds. In the inset, n denotes the number of C (carbon) and O (oxygen) atoms in HAT_{*n*} molecules.

the output transient photocurrent curves were obtained to estimate the transit time (τ_{tr}) of the charge carriers. Figure 5 (a) represents the transient photocurrent curves with the estimated transit time of the charge carriers for the HAT4, HAT5, HAT6 and HAT8 compounds at 80 °C by applying the bias of 20 V. Depending on the nature of material and charge transport mechanism, one can obtain various shapes in the transient photocurrent curves. Herein, for the investigated HAT_{*n*} compounds, we have recorded a plateau level in the photocurrent curves which is designated to a typical non-dispersive transient behaviour, as clearly visible in Figure 5 (a). This non-dispersive transient nature of the photocurrent curve is analogous to the bulk photogeneration of charge carriers. Such nature of photocurrent curve also provides information about the absence of prominent trapping sites and effective contribution of space charges [48]. In general, the mobility can be calculated from the ToF signal and corresponding transit time using equation 1. In the present investigation, we have used a more accurate method to cal-

culate the mobility of holes in the HAT_{*n*} compounds. By applying different bias voltages, we plotted the drift velocity versus electric field curve and the hole mobility was determined from the slope of the linearly fitted curve according to the relation: $v = \mu \cdot E$. In order to acquire ToF signal with clear plateau, we apply appropriate voltage range of 5–25V, 15–35V, 20–60V and 30–70V for the HAT4, HAT5, HAT6 and HAT8, respectively. Figure 5 (b) shows the linear fitting of the drift velocity versus electric field curves of the HAT_{*n*} at 80 °C.

Figure 6 (a) illustrates the variation of hole mobility as a function of temperature for the HAT_{*n*} compounds. Within the regime of hexagonal columnar mesophase of the triphenylene-based DLCs, it is generally perceived that the hole mobility remains temperature invariant [39, 31, 51]. We have confirmed almost temperature invariant hole mobility in the HAT_{*n*} compounds as shown in Figure 6(a). This manifests that the columnar molecular assemblies in the HAT_{*n*} compounds are unidirectionally oriented and the self assemblies remain intact with the variation in temperature for the entire mesophase. For HAT4, the average hole mobility was found to be 1.216×10^{-2} and 0.6×10^{-2} cm²V⁻¹s⁻¹ in the columnar plastic and crystalline intermediate phase, respectively. The HAT4 compound exhibits higher mobility as compared to the HAT5, HAT6 and HAT8 due to its superior column ordering with respect to other HAT_{*n*} homologues. The average hole mobilities for the HAT5, HAT6 and HAT8 were found to be 2.27×10^{-3} , 4.86×10^{-4} and 1.7×10^{-4} cm²V⁻¹s⁻¹, respectively. As we mentioned previously, that the value of mobility significantly depends on molecular ordering; consequently, we have noticed higher mobility for the HAT5 compound as compared to our previously reported article [52]. This has been achieved due to very slow cooling of the compounds with a rate of 0.01 °C/min from the isotropic phase. As the alkyl chain length in the HAT_{*n*} compounds increases, the inter-columnar and intra-columnar ordering decreases leading to a lower mobility value for holes. The complete mechanism can be understood via short-range electrostatic interactions that defines the molecular packing. As the alkyl group R increases from C₄H₉ to C₈H₁₇, the strength of electrostatic interaction decreases; subsequently, molecular packing becomes weaker resulting in a lower molecular ordering on going from HAT4 to HAT8.

In 2001, van de Craats *et al.* proposed the following empirical relationship [49] for explaining the behaviour of mobility with increasing size of different macrocyclic cores containing C, O, and N atoms;

$$\sum \mu \approx a.exp(-b/n). \quad (3)$$

In this expression, $\sum \mu$ is a mobility sum for holes and electrons along the axis of the column and n represents the total number of C, O and N atoms in the aromatic core. The experimental results of mobility $\sum \mu$ used by the authors were obtained by the time-resolved microwave conductivity

Compound	n	a (cm ² /Vs)	b	Method	Reference
Different discotic LCs	Total number of C, O, and N in the core	3	83	PR-TRMC	[49], [50]
HAT _{<i>n</i>}	Total number of C atoms in the alkyl chain	$2.33 \pm 0.51 \times 10^{-6}$	-205.70 ± 5.4	ToF	Present work
HAT _{<i>n</i>}	Total number of C and O atoms in the molecule	$3.27 \pm 0.72 \times 10^{-9}$	-726.69 ± 11	ToF	Present work

Table 2

Mobility fitting parameters using relationship (3). In reference 47, the molecules cores contain C, O and N atoms, whereas in reference 48 the cores contain only C atoms.

(PR-TRMC) technique where the examined mobility is collectively subjected to positive and negative charge carriers. They have demonstrated that the maximum mobility shows a linear semi-logarithmic dependence on $1/n$, and the values of constants a and b were found to be 3 and 83, respectively. The increasing mobility with the increase in core size was assigned due to the electronic coupling between the p-orbitals of adjacent macrocycles and an increased cohesive force between the macrocycles via van der Waals and electrostatic interactions. Van de Craats *et al.* [49] have used the equation (3) for mobility analysis of the DLCs with increasing core sizes corresponding to values of n between 18 and 42. Later on, Debije *et al.* [50] have employed the same relationship to analyze mobility for other DLCs with polycyclic aromatic cores containing carbon atoms only. They concluded that equation (3) can be used only for limited values of n ; the experimental data have shown that the mobility is relatively insensitive to size of the aromatic core for $n > 40$. In the present work, we have generalized equation (3) to include the influence of lateral chain length on the hole mobility. To the best of our knowledge, none has scrutinized the validity of this empirical formula over the results acquired by the time-of-flight technique in which hole or electron mobility can be evaluated separately. As HAT_{*n*} consists of the same core size and only differs in the attached peripheral chain; we have considered two different aspects for n . First, we did fitting of the mobility of HAT_{*n*} using equation (3) by taking only the number of carbon atoms in the alkyl chain; as shown in Figure 6(b), the formula matches very well with experimental data. The negative value of b is due to the decrease in mobility with increasing alkyl chain length in contrast to the core size effect which leads to a positive value of b . Later on, we have also fitted the experimental data of HAT_{*n*} by considering the number of C and O atoms in the core and alkyl chain; the values of a and b deduced from the different fits have been summarized in Table 2. Furthermore, the effect of the disorder introduced with the longer alkyl chain contribute to the decrease in mobility.

3.4. Dielectric spectroscopy

Dielectric response is subtle to molecular dipole moment orientation with respect to the applied external electric field. Consequently, the dielectric properties of liquid crystals depends on molecular ordering and sample orientation relative to the measuring electric field [53]. Recently, Yildirim *et al.* [54] utilized dielectric spectroscopy to investigate the collective orientational ordering of HAT6 under nanoscale confinement. To make this technique as useful as possi-

ble; the characterization should be carried out over a wide frequency range in order to clearly distinguish the different mechanism which can be deduced from the dielectric spectrum (static dielectric permittivity, dielectric relaxations and DC conductivity contribution). In the present work, the real (ϵ') and imaginary (ϵ'') parts of the complex dielectric permittivity (ϵ^*) were measured in the frequency range of 20 Hz-1 MHz. The dielectric measurements have been done by applying temperature scans with cooling rate of 0.2 °C/min. Figure 7 depicts an example of dielectric spectra obtained in the columnar hexagonal phase of HAT5. Similar spectra can be perceived for the HAT4, HAT6 and HAT8. The real part of the complex dielectric permittivity (ϵ') manifests a constant value corresponding to the static dielectric permittivity limit. At lower frequencies, ϵ' increases, which is attributed to the contribution from DC conductivity (σ). The imaginary part, ϵ'' also provides the contribution of σ in the lower frequency region. At higher frequencies, the increase of ϵ'' is linked with the ITO resistivity of the sample cell.

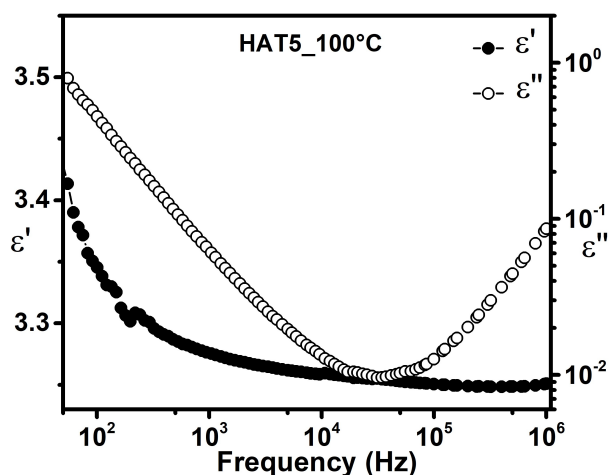


Figure 7: Frequency dependency of dielectric permittivity and dielectric loss of the HAT5 compound at 100 °C.

Dielectric spectroscopy is insufficient to provide the liquid crystalline phase structure; however, it evinces a deep understanding of the molecular ordering and average orientation of dipole moments which makes this technique useful to investigate the change in ordering during phase transitions. [48]. Figure 8 (a) shows the temperature dependence of static permittivity for the HAT5 determined at static frequency of 3kHz. The jump observed at $T_{Col-I} = 122^\circ\text{C}$ on the $\epsilon'(T)$ curve corresponds to ordering change at the transi-

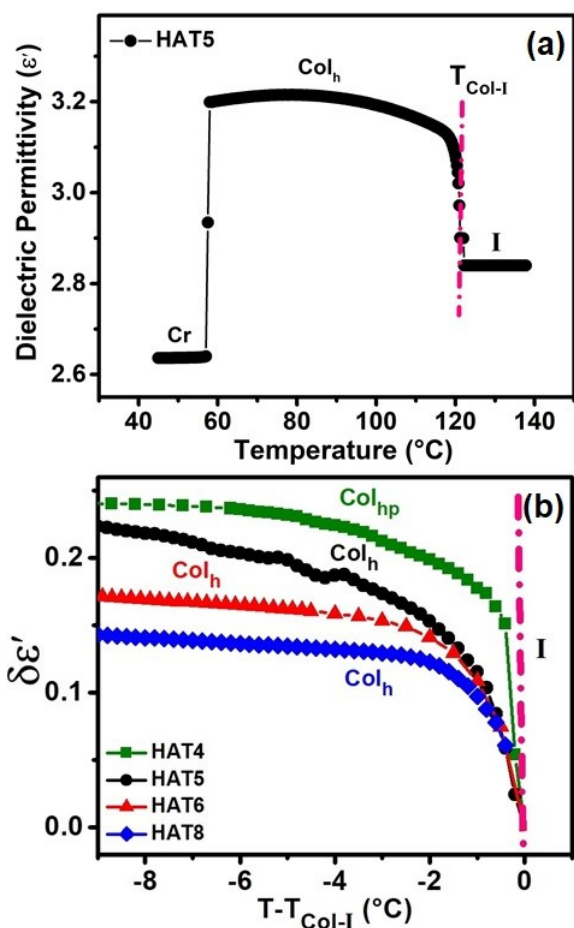


Figure 8: (a) Static dielectric permittivity of HAT5 as a function of temperature from the isotropic to crystalline phase in the cooling cycle; (b) Variation of the excess static dielectric permittivity from isotropic to columnar phase as function of shifted temperature for HAT4, HAT5, HAT6 and HAT8. The values of ϵ' were determined at 3 kHz from the dielectric spectra.

tion between the isotropic and columnar phases. Transition temperatures deduced from $\epsilon'(T)$ curve are slightly different when compared to DSC measurements. This is due to the different cooling rates and sample preparation techniques. In the columnar phase, the ordering and homeotropic alignment of the sample promote the coupling between the dipole moment and the applied electric field; which in turn, increases the measured permittivity. The dielectric response is principally due to the dipole moments of alkoxy group, which is of 1.28 D at an angle of 72° with the C-O bond; the alkoxy groups rotate freely, which allows a dipole orientation under an electric field. The dynamics of the core and the alkoxy groups are strongly correlated; consequently, the orientation of the alkoxy group remains involved with the core motion [55].

The change of ϵ' from isotropic (ϵ'_I) to columnar (ϵ'_{Col}) phase corresponds to the change in ordering between the two phases. We define here the excess permittivity, $\delta\epsilon' =$

$\epsilon'_{Col} - \epsilon'_I$, as the difference between the temperature dependence of ϵ'_{Col} and that of ϵ'_I . In Figure 8 (b), we report $\delta\epsilon'$ as a function of temperature for HAT_n compounds. The sudden increase of $\delta\epsilon'$ at T_{Col-I} indicates that the columns are oriented perpendicularly to the electrodes, as observed by POMs. $\delta\epsilon'$ can also be used to compare molecular ordering in the columnar phase of different HAT_n compounds. From Figure 8 (b), we can observe that near T_{Col-I} temperature $\delta\epsilon'$ is the highest for HAT4 and decreases with increasing the alkyl chain length. These results can be explained by the lowering of molecular ordering within the columns, when the number (*n*), of carbon atoms in the alkyl chain increases. We can perceive the effect of the disordering in the HAT_n compounds from Figure 9 (a) in which the exponential decrease in the $\delta\epsilon'$ is observed with increasing the number of carbon atoms in the alkyl chain at the vicinity of the Col-I transition. This exponential tendency is similar to that obtained for entropy changes, $\Delta S_{Col-I} = \Delta H_{Col-I} / T_{Col-I}$, associated to Col-I transition (Figure 9 (b)). ΔS_{Col-I} can be regarded as a fundamental characteristic that is representative of changes of molecular order at phase transition. ΔS_{Col-I} data were deduced from DSC measurements of the enthalpy changes, ΔH_{Col-I} at T_{Col-I} (Table 1). The exponential decrease of ΔS_{Col-I} with *n* is consistent with our interpretation that the discotic molecules have more degree of freedom within columns leading to a more disordered phase and hence to the increase of the entropy. The common exponential decrease with *n* of the different physical parameters $\delta\epsilon'$, ΔS_{Col-I} as well as the hole mobility (Figure 6 (b)), based on three different techniques are consistent and coherent with the interpretation that the charge transport along the column axis is strongly correlated to the degree of molecular ordering within the columns.

4. Conclusions

In summary, the molecular ordering dependent charge transport in π -stacked triphenylene based discotic liquid crystals has been investigated. The homologous members of HAT_n were characterized by various techniques like differential scanning calorimetry, polarized optical microscopy, UV-visible spectroscopy, dielectric spectroscopy and time-of-flight. In this study, the HAT_n (*n* = 5, 6 and 8) render the hexagonal columnar phase (Col_h), whereas the compound HAT4 exhibits columnar plastic phase (Col_{hp}) along with the crystalline intermediate phase (Cr'). The DSC revealed that the Col_h -isotropic phase transition temperature for HAT_n increases with decreasing length of peripheral alkyl chain due to structure-property relationship. The Col_{hp} and Col_h phases were recognized via mini mosaic and classical dendritic optical textures. The HAT_n compounds yield an absorption peak about 350 nm which was attributed to the π - π^* transitions in C=C bonds of the triphenylene core. We observed that the absorbance decreases with increasing alkyl chain length which is probably due to the inductive effect of the stabilizing carbocation mechanism. The charge transport phenomenon in the HAT_n compounds scrutinized by

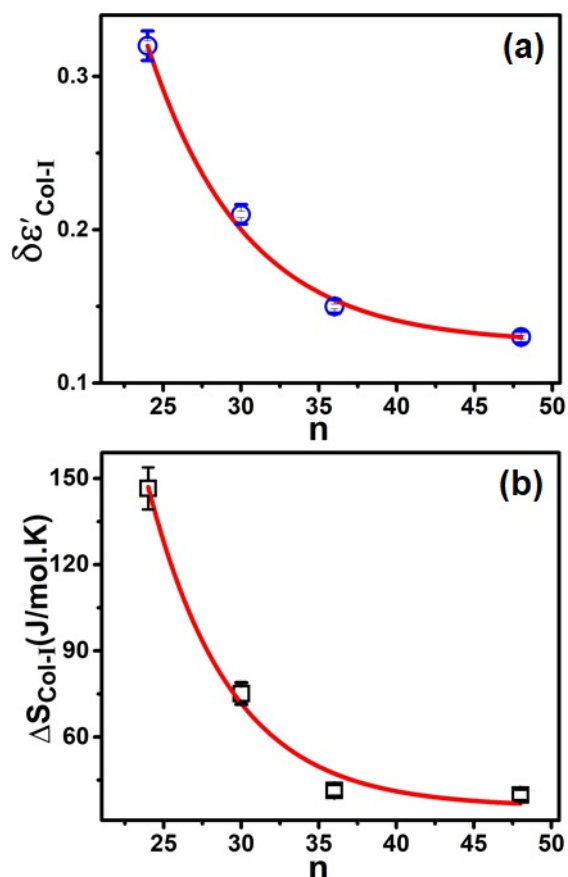


Figure 9: (a) Excess static dielectric permittivity and (b) Entropy changes as a function of number of carbon atoms in the alkyl chain of the HAT_n compounds at T_{Col-I} .

evaluating the hole mobility using the time-of-flight technique. The HAT_n compounds show non-dispersive transient nature in the photocurrent curves. The HAT4 compound exhibits higher mobility as compared to the HAT5, HAT6 and HAT8 due to its superior molecular ordering with respect to other HAT_n homologous. The average hole mobilities for the HAT5, HAT6 and HAT8 were found to be 2.27×10^{-3} , 4.86×10^{-4} and 1.7×10^{-4} $\text{cm}^2\text{V}^{-1}\text{s}^{-1}$ in the hexagonal columnar phase; whereas, for the HAT4, the hole mobility was found to be 1.216×10^{-2} and 0.6×10^{-2} $\text{cm}^2\text{V}^{-1}\text{s}^{-1}$ in the columnar plastic and crystalline intermediate phases, respectively. The variation of the hole mobility versus alkyl chain length was fitted using the empirical formula $\mu \approx a.exp(-b/n)$, where n is the number of carbon atoms in the alkyl chain; the formula also matches with experimental data when we consider n as the total number of carbon and oxygen atoms. Usually, the mobility depends on the molecular ordering in the columnar matrix. The change in hole mobility in combination with molecular ordering could be understood via short-range electrostatic interactions that define the molecular packing. As the alkyl group, R , increases from C_4H_9 to C_8H_{17} , the strength of electrostatic interaction decreases; subsequently, molecular packing becomes weaker resulting in a lower molecular or-

dering in the HAT8 in comparison to HAT4. The change in molecular ordering was further confirmed by dielectric spectroscopy; the variation of $\delta\epsilon'_{I-Col}$ (change in dielectric permittivity at the isotropic to columnar phase transition) is highest for the HAT4 and decreases with increasing alkyl chain length. The disordering in the HAT compounds was

further investigated by explaining the change in entropy with increase in alkyl chain length. HAT_n homologous show their potential applications as organic semiconductors.

Conflicts of interest

“There are no conflicts to declare”.

Acknowledgements

AS is thankful to the Région, Hauts de France and Pôle Métropolitain Côte d’Opale (PMCO) for the financial assistance. Prof. A. Hadj Sahraoui, the Director of UDSMM is gratefully acknowledged for his kind support and encouragement.

References

- [1] S. Sergeyev, W. Pisula, Y. H. Geerts, Discotic liquid crystals: a new generation of organic semiconductors, *Chemical Society Reviews* 36 (2007) 1902–1929. URL: <http://pubs.rsc.org/en/content/articlelanding/2007/cs/b417320c>. doi:10.1039/B417320C.
- [2] S. Kumar, Self-organization of disc-like molecules: chemical aspects, *Chemical Society Reviews* 35 (2006) 83–109. URL: <https://pubs.rsc.org/en/content/articlelanding/2006/cs/b506619k>. doi:10.1039/B506619K.
- [3] S. Laschat, A. Baro, N. Steinke, F. Giesselmann, C. Hägele, G. Scalia, R. Judele, E. Kapatsina, S. Sauer, A. Schreivogel, M. Tosoni, Discotic Liquid Crystals: From Tailor-Made Synthesis to Plastic Electronics, *Angewandte Chemie International Edition* 46 (2007) 4832–4887. URL: <https://onlinelibrary.wiley.com/doi/abs/10.1002/anie.200604203>. doi:10.1002/anie.200604203.
- [4] V. S. K. Balagurusamy, S. K. Prasad, S. Chandrasekhar, S. Kumar, M. Manickam, C. V. Yelamaggad, Quasi-one dimensional electrical conductivity and thermoelectric power studies on a discotic liquid crystal, *Pramana* 53 (1999) 3–11. doi:<https://doi.org/10.1007/s12043-999-0136-2>.
- [5] R. J. Bushby, O. R. Lozman, Photoconducting liquid crystals, *Current Opinion in Solid State and Materials Science* 6 (2002) 569 – 578. URL: <http://www.sciencedirect.com/science/article/pii/S135902860300007X>. doi:[https://doi.org/10.1016/S1359-0286\(03\)00007-X](https://doi.org/10.1016/S1359-0286(03)00007-X).
- [6] B. R. Kaafarani, Discotic Liquid Crystals for Opto-Electronic Applications, *Chemistry of Materials* 23 (2011) 378–396. URL: <https://doi.org/10.1021/cm102117c>. doi:10.1021/cm102117c.
- [7] N. Boden, R. J. Bushby, J. Clements, Mechanism of quasi-one-dimensional electronic conductivity in discotic liquid crystals, *The Journal of Chemical Physics* 98 (1993) 5920–5931. URL: <https://aip.scitation.org/doi/abs/10.1063/1.464886>. doi:10.1063/1.464886.
- [8] M. Kumar, S. Kumar, Liquid crystals in photovoltaics: a new generation of organic photovoltaics, *Polymer Journal* 49 (2017) 85–111. URL: <https://www.nature.com/articles/pj2016109>. doi:10.1038/pj.2016.109.
- [9] M. Lehmann, G. Kestemont, R. Gomez Aspe, C. Buess-Herman, M. H. J. Koch, M. G. Debije, J. Piris, M. P. de Haas, J. M. Warman, M. D. Watson, V. Lemaur, J. Cornil, Y. H. Geerts,

- R. Gearba, D. A. Ivanov, High Charge-Carrier Mobility in +- Deficient Discotic Mesogens: Design and Structure-Property Relationship, *Chemistry – A European Journal* 11 (2005) 3349–3362. URL: <https://chemistry-europe.onlinelibrary.wiley.com/doi/abs/10.1002/chem.200400586>. doi:10.1002/chem.200400586.
- [10] V. Lemaire, D. A. da Silva Filho, V. Coropceanu, M. Lehmann, Y. Geerts, J. Piris, M. G. Debije, A. M. van de Craats, K. Senthilkumar, L. D. A. Siebbeles, J. M. Warman, J.-L. Brédas, J. Cornil, Charge Transport Properties in Discotic Liquid Crystals: A Quantum-Chemical Insight into Structure-Property Relationships, *Journal of the American Chemical Society* 126 (2004) 3271–3279. URL: <https://doi.org/10.1021/ja0390956>. doi:10.1021/ja0390956.
- [11] I. Bala, W.-Y. Yang, S. P. Gupta, J. De, R. A. K. Yadav, D. P. Singh, D. K. Dubey, J.-H. Jou, R. Douali, S. K. Pal, Room temperature discotic liquid crystalline triphenylene-pentaalkynylbenzene dyads as an emitter in blue OLEDs and their charge transfer complexes with ambipolar charge transport behaviour, *Journal of Materials Chemistry C* 7 (2019) 5724–5738. URL: <https://pubs.rsc.org/en/content/articlelanding/2019/tc/c9tc01178a>. doi:10.1039/C9TC01178A.
- [12] F. Würthner, C. Thalacker, S. Diele, C. Tschierske, Fluorescent J-type Aggregates and Thermotropic Columnar Mesophases of Perylene Bisimide Dyes, *Chemistry – A European Journal* 7 (2001) 2245–2253. URL: [https://chemistry-europe.onlinelibrary.wiley.com/doi/abs/10.1002/1521-3765\(20010518\)7:3A10%3C2245%3A3AAID-CHEM2245%3E3.0.CO%3B2-W](https://chemistry-europe.onlinelibrary.wiley.com/doi/abs/10.1002/1521-3765(20010518)7:3A10%3C2245%3A3AAID-CHEM2245%3E3.0.CO%3B2-W). doi:10.1002/1521-3765(20010518)7:3A10%3C2245%3E3.0.CO%3B2-W.
- [13] B. A. Gregg, M. A. Fox, A. J. Bard, Photovoltaic effect in symmetrical cells of a liquid crystal porphyrin, *The Journal of Physical Chemistry* 94 (1990) 1586–1598. URL: <https://doi.org/10.1021/j100367a068>. doi:10.1021/j100367a068.
- [14] L. Schmidt-Mende, A. Fechtenkötter, K. Müllen, E. Moons, R. H. Friend, J. D. MacKenzie, Self-Organized Discotic Liquid Crystals for High-Efficiency Organic Photovoltaics, *Science* 293 (2001) 1119–1122. URL: <https://science.sciencemag.org/content/293/5532/1119>. doi:10.1126/science.293.5532.1119.
- [15] X. Chen, L. Chen, Y. Chen, Self-assembly of discotic liquid crystal decorated ZnO nanoparticles for efficient hybrid solar cells, *RSC Adv.* 4 (2014) 3627–3632. URL: <http://dx.doi.org/10.1039/C3RA44980G>. doi:10.1039/C3RA44980G.
- [16] A. Bacher, I. Bleyl, C. H. Erdelen, D. Haarer, W. Paulus, H.-W. Schmidt, Low molecular weight and polymeric triphenylenes as hole transport materials in organic two-layer LEDs, *Advanced Materials* 9 (1997) 1031–1035. URL: <https://onlinelibrary.wiley.com/doi/abs/10.1002/adma.19970091307>. doi:10.1002/adma.19970091307.
- [17] J. H. Wendorff, T. Christ, B. Glösen, A. Greiner, A. Kettner, R. Sander, V. Stümpflen, V. V. Tsukruk, Columnar discotics for light emitting diodes, *Advanced Materials* 9 (1997) 48–52. URL: <https://onlinelibrary.wiley.com/doi/abs/10.1002/adma.19970090110>. doi:10.1002/adma.19970090110.
- [18] I. O. Shklyarevskiy, P. Jonkheijm, N. Stutzmann, D. Wasserberg, H. J. Wondergem, P. C. M. Christianen, A. P. H. J. Schenning, D. M. de Leeuw, V. Tomović, J. Wu, K. Müllen, J. C. Maan, High Anisotropy of the Field-Effect Transistor Mobility in Magnetically Aligned Discotic Liquid-Crystalline Semiconductors, *Journal of the American Chemical Society* 127 (2005) 16233–16237. URL: <https://doi.org/10.1021/ja054694t>. doi:10.1021/ja054694t.
- [19] R. J. Bushby, K. Kawata, Liquid crystals that affected the world: discotic liquid crystals, *Liquid Crystals* 38 (2011) 1415–1426. URL: <https://doi.org/10.1080/02678292.2011.603262>. doi:10.1080/02678292.2011.603262.
- [20] D. Markovitsi, A. Germain, P. Millie, P. Lecuyer, L. Gallos, P. Argyrakis, H. Bungs, H. Ringsdorf, Triphenylene Columnar Liquid Crystals: Excited States and Energy Transfer, *The Journal of Physical Chemistry* 99 (1995) 1005–1017. URL: <https://doi.org/10.1021/j100003a025>. doi:10.1021/j100003a025.
- [21] S. FORGET, H. S. KITZEROW, Preliminary communication Optical storage effect in a discotic columnar liquid crystal, *Liquid Crystals* 23 (1997) 919–922. URL: <https://doi.org/10.1080/026782997207867>. doi:10.1080/026782997207867.
- [22] N. Boden, R. J. Bushby, J. Clements, B. Movaghar, Device applications of charge transport in discotic liquid crystals, *Journal of Materials Chemistry* 9 (1999) 2081–2086. URL: <https://pubs.rsc.org/en/content/articlelanding/1999/jm/a903005k>. doi:10.1039/A903005K.
- [23] J.-i. Hanna, *Liquid Crystalline Semiconductors*, volume 169, Springer Netherlands, 2012. URL: https://doi.org/10.1007/2F978-90-481-2873-0_2.
- [24] C. Destradé, M. C. Mondon, J. Malthete, HEXASUBSTITUTED TRIPHENYLENES : A NEW MESOMORPHIC ORDER, *Le Journal de Physique Colloques* 40 (1979) C3–17–C3–21. URL: <http://dx.doi.org/10.1051/jphyscol:1979305>. doi:10.1051/jphyscol:1979305.
- [25] S. Kumar, Triphenylene-based discotic liquid crystal dimers, oligomers and polymers, *Liquid Crystals* 32 (2005) 1089–1113. URL: <https://doi.org/10.1080/02678290500117415>. doi:10.1080/02678290500117415.
- [26] M. A. Palenberg, R. J. Silbey, M. Malagoli, J.-L. Brédas, Almost temperature independent charge carrier mobilities in liquid crystals, *The Journal of Chemical Physics* 112 (2000) 1541–1546. URL: <https://aip.scitation.org/doi/abs/10.1063/1.480700>. doi:10.1063/1.480700.
- [27] T. Kreouzis, K. J. Donovan, N. Boden, R. J. Bushby, O. R. Lozman, Q. Liu, Temperature-independent hole mobility in discotic liquid crystals, *The Journal of Chemical Physics* 114 (2001) 1797–1802. URL: <https://doi.org/10.1063/1.1334958>. doi:10.1063/1.1334958.
- [28] V. Duzhko, A. Semyonov, R. J. Twieg, K. D. Singer, Correlated polaron transport in a quasi-one-dimensional liquid crystal, *Physical Review B* 73 (2006) 064201. URL: <https://link.aps.org/doi/10.1103/PhysRevB.73.064201>. doi:10.1103/PhysRevB.73.064201, publisher: American Physical Society.
- [29] H. K. Bisoyi, S. Kumar, Discotic nematic liquid crystals: science and technology, *Chemical Society Reviews* 39 (2009) 264–285. URL: <https://pubs.rsc.org/en/content/articlelanding/2010/cs/b901792p>. doi:10.1039/B901792P, publisher: The Royal Society of Chemistry.
- [30] D. Adam, F. Closs, T. Frey, D. Funhoff, D. Haarer, P. Schumacher, K. Siemensmeyer, Transient photoconductivity in a discotic liquid crystal, *Phys. Rev. Lett.* 70 (1993) 457–460. URL: <https://link.aps.org/doi/10.1103/PhysRevLett.70.457>. doi:10.1103/PhysRevLett.70.457.
- [31] H. Iino, J.-i. Hanna, D. Haarer, Electronic and ionic carrier transport in discotic liquid crystalline photoconductor, *Physical Review B* 72 (2005) 193203. URL: <https://link.aps.org/doi/10.1103/PhysRevB.72.193203>. doi:10.1103/PhysRevB.72.193203.
- [32] A. Gowda, L. Jacob, D. P. Singh, R. Douali, S. Kumar, Charge Transport in Novel Phenazine Fused Triphenylene Supramolecular Systems, *ChemistrySelect* 3 (2018) 6551–6560. URL: <https://onlinelibrary.wiley.com/doi/abs/10.1002/slct.201801412>. doi:10.1002/slct.201801412.
- [33] P. Mahesh, A. Shah, K. Swamynathan, D. P. Singh, R. Douali, S. Kumar, Carbon dot-dispersed hexabutyloxytriphenylene discotic mesogens: structural, morphological and charge transport behavior, *Journal of Materials Chemistry C* 8 (2020) 9252–9261. URL: <https://pubs.rsc.org/en/content/articlelanding/2020/tc/d0tc02028a>. doi:10.1039/D0TC02028A, publisher: The Royal Society of Chemistry.
- [34] S. Paul, B. Ellman, S. Tripathi, G. Singh, R. J. Twieg, Development of a scanning time of flight microscope and its application to the study of charge transport in phase separated structured organic semiconductors, *Journal of Applied Physics* 119 (2016) 145501. URL: <https://aip.scitation.org/doi/abs/10.1063/1.4945429>. doi:10.1063/1.4945429, publisher: American Institute of Physics.
- [35] A. Khare, R. Uttam, S. Kumar, R. Dhar, Enhanced charge carrier conduction and other characteristic parameters of hexagonal plastic columnar phase of a discotic liquid crystalline material due to functionalized gold nanoparticles, *Journal of Molecular Liquids* 317 (2020) 113985. URL: <https://www.sciencedirect.com/science/article/pii/S0167732220342744>. doi:10.1016/j.molliq.2020.113985.
- [36] S. Kumar, *Chemistry of Discotic Liquid Crystals: From Monomers to Polymers*, 2010. URL: <https://www.crcpress.com/>

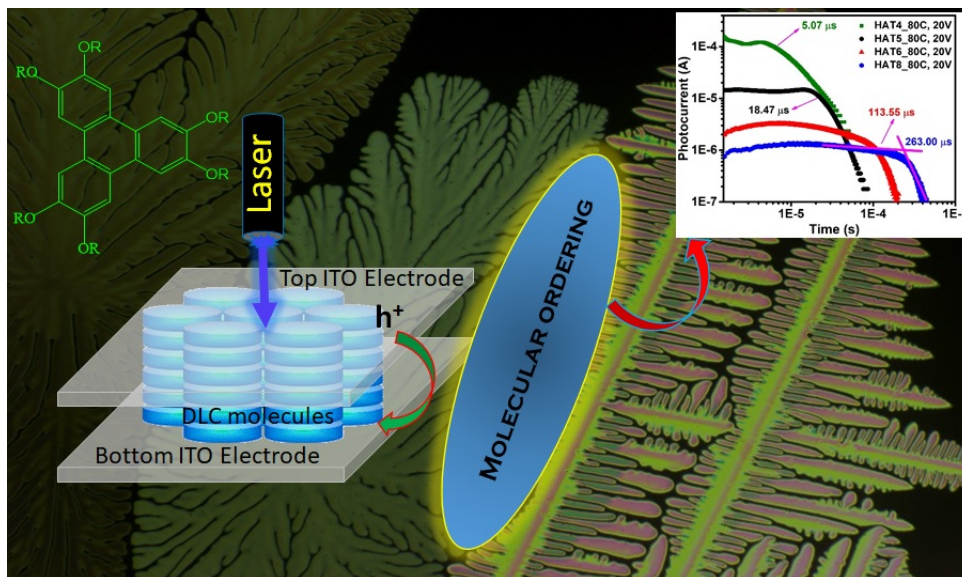
Chemistry-of-Discotic-Liquid-Crystals-From-Monomers-to-Polymers/
Kumar/p/book/9781439811436.

- [37] P. J. Stackhouse, M. Hird, Influence of branched chains on the mesomorphic properties of symmetrical and unsymmetrical triphenylene discotic liquid crystals, *Liquid Crystals* 35 (2008) 597–607. URL: <https://doi.org/10.1080/02678290802040026>. doi:10.1080/02678290802040026.
- [38] Y. Hirai, H. Monobe, N. Mizoshita, M. Moriyama, K. Hanabusa, Y. Shimizu, T. Kato, Enhanced Hole-Transporting Behavior of Discotic Liquid-Crystalline Physical Gels, *Advanced Functional Materials* 18 (2008) 1668–1675. URL: <https://onlinelibrary.wiley.com/doi/abs/10.1002/adfm.200701313>. doi:10.1002/adfm.200701313.
- [39] H. Bengs, F. Closs, T. Frey, D. Funhoff, H. Ringsdorf, K. Siemensmeyer, Highly photoconductive discotic liquid crystals Structure–property relations in the homologous series of hexa-alkoxytriphenylenes, *Liquid Crystals* 15 (1993) 565–574. URL: <https://doi.org/10.1080/02678299308036478>. doi:10.1080/02678299308036478.
- [40] H. Monobe, Y. Shimizu, S. Okamoto, H. Enomoto, Ambipolar Charge Carrier Transport Properties in the Homologous Series of 2,3,6,7,10,11-hexaalkoxytriphenylene, *Molecular Crystals and Liquid Crystals* 476 (2007) 31/[277]–41/[287]. URL: <https://doi.org/10.1080/15421400701732324>. doi:10.1080/15421400701732324.
- [41] I. Dierking, *Textures of Liquid Crystals*, Wiley - VCH Verlag GmbH & CO. KGaA, 2003. URL: [https://www.research.manchester.ac.uk/portal/en/publications/textures-of-liquid-crystals\(b7d4f4ba-93ca-4540-a8b0-3119de2a094c\)/export.html](https://www.research.manchester.ac.uk/portal/en/publications/textures-of-liquid-crystals(b7d4f4ba-93ca-4540-a8b0-3119de2a094c)/export.html).
- [42] H. Monobe, H. Hori, Y. Shimizu, K. Awazu, Alignment Control of Columnar Liquid Crystals for Uniformly Homeotropic Domain with Circularly Polarized Infrared Irradiation, *Molecular Crystals and Liquid Crystals* 475 (2007) 13–22. URL: <https://doi.org/10.1080/15421400701732332>. doi:10.1080/15421400701732332.
- [43] H. K. Bisoyi, S. Kumar, Microwave-assisted facile synthesis of liquid crystalline non-symmetrical hexaalkoxytriphenylenes containing a branched chain and their characterization, *Journal of Physical Organic Chemistry* 21 (2008) 47–52. URL: <https://onlinelibrary.wiley.com/doi/abs/10.1002/poc.1283>. doi:10.1002/poc.1283.
- [44] P. Yaduvanshi, S. Kumar, R. Dhar, Effects of copper nanoparticles on the thermodynamic, electrical and optical properties of a disc-shaped liquid crystalline material showing columnar phase, *Phase Transitions* 88 (2015) 489–502. URL: <https://doi.org/10.1080/01411594.2014.984710>. doi:10.1080/01411594.2014.984710.
- [45] T. G. Mayerhöfer, A. V. Pipa, J. Popp, Beer's Law-Why Integrated Absorbance Depends Linearly on Concentration, *ChemPhysChem* 20 (2019) 2748–2753. URL: <https://chemistry-europe.onlinelibrary.wiley.com/doi/abs/10.1002/cphc.201900787>. doi:10.1002/cphc.201900787.
- [46] T. G. Mayerhöfer, J. Popp, Beer's Law – Why Absorbance Depends (Almost) Linearly on Concentration, *ChemPhysChem* 20 (2019) 511–515. URL: <https://chemistry-europe.onlinelibrary.wiley.com/doi/abs/10.1002/cphc.201801073>. doi:10.1002/cphc.201801073.
- [47] D. J. S. Sandbeck, D. J. Markewich, A. L. L. East, The Carbocation Rearrangement Mechanism, Clarified, *The Journal of Organic Chemistry* 81 (2016) 1410–1415. URL: <https://doi.org/10.1021/acs.joc.5b02553>. doi:10.1021/acs.joc.5b02553.
- [48] A. Shah, B. Duponchel, A. Gowda, S. Kumar, M. Becuwe, C. Davoisne, C. Legrand, R. Douali, D. P. Singh, Charge transport in phenazine-fused triphenylene discotic mesogens doped with CdS nanowires, *New Journal of Chemistry* (2020). URL: <https://pubs.rsc.org/en/content/articlelanding/2020/nj/d0nj03290e>. doi:10.1039/D0NJ03290E, publisher: The Royal Society of Chemistry.
- [49] A. M. van de Craats, J. M. Warman, The Core-Size Effect on the Mobility of Charge in Discotic Liquid Crystalline Materials, *Advanced Materials* 13 (2001) 130–133. URL: <https://onlinelibrary.wiley.com/doi/10.1002/1521-4095.28200101%2913%3A2%3C130%3A%3AAID-ADMA130%3E3.0.CO%3B2-L>. doi:10.1002/1521-4095(200101)13:2<130::AID-ADMA130>3.0.CO;2-L.
- [50] M. G. Debije, J. Piris, M. P. de Haas, J. M. Warman, e. Tomović, C. D. Simpson, M. D. Watson, K. Müllen, The Optical and Charge Transport Properties of Discotic Materials with Large Aromatic Hydrocarbon Cores, *Journal of the American Chemical Society* 126 (2004) 4641–4645. URL: <https://doi.org/10.1021/ja0395994>. doi:10.1021/ja0395994, publisher: American Chemical Society.
- [51] H. Iino, J.-i. Hanna, D. Haarer, R. J. Bushby, Fast Electron Transport in Discotic Columnar Phases of Triphenylene Derivatives, *Japanese Journal of Applied Physics* 45 (2006) 430–433. URL: <https://doi.org/10.1143/JJAP.45.430>. doi:10.1143/JJAP.45.430.
- [52] K. Kondratenko, D. P. Singh, Y. Boussoualem, R. Douali, C. Legrand, A. Daoudi, Hole transporting properties of discotic liquid-crystalline semiconductor confined in calamitic UV-crosslinked gel, *Journal of Molecular Liquids* 276 (2019) 27 – 31. URL: <http://www.sciencedirect.com/science/article/pii/S0167732218351559>. doi:https://doi.org/10.1016/j.molliq.2018.11.137.
- [53] H. Groothues, F. Kremer, D. M. Collard, C. P. Lillya, Dynamic properties of discotic liquid crystals with triphenylene and benzene cores, studied by broadband dielectric spectroscopy, *Liquid Crystals* 18 (1995) 117–121. URL: <https://doi.org/10.1080/02678299508036600>. doi:10.1080/02678299508036600.
- [54] A. Yildirim, A. Bühlmeier, S. Hayashi, J. C. Haenle, K. Sentker, C. Krause, P. Huber, S. Laschat, A. Schönhals, Multiple glassy dynamics in dipole functionalized triphenylene-based discotic liquid crystals revealed by broadband dielectric spectroscopy and advanced calorimetry – assessment of the molecular origin, *Physical Chemistry Chemical Physics* 21 (2019) 18265–18277. URL: <https://pubs.rsc.org/en/content/articlelanding/2019/cp/c9cp03499d>. doi:10.1039/C9CP03499D, publisher: The Royal Society of Chemistry.
- [55] F. M. Mulder, J. Stride, S. J. Picken, P. H. J. Kouwer, M. P. de Haas, L. D. A. Siebbeles, G. J. Kearley, Dynamics of a Triphenylene Discotic Molecule, HAT6, in the Columnar and Isotropic Liquid Phases, *Journal of the American Chemical Society* 125 (2003) 3860–3866. URL: <https://doi.org/10.1021/ja029227f>. doi:10.1021/ja029227f.

Graphical Abstract

Molecular ordering dependent charge transport in π -stacked triphenylene based discotic liquid crystals and its correlation with dielectric properties

Asmita Shah, Dharmendra Pratap Singh, Benoit Duponchel, Freddy Krasinski, Abdelylah Daoudi, Sandeep Kumar, Redouane Douali



Highlights

Molecular ordering dependent charge transport in π -stacked triphenylene based discotic liquid crystals and its correlation with dielectric properties

Asmita Shah, Dharmendra Pratap Singh, Benoit Duponchel, Freddy Krasisnski, Abdelylah Daoudi, Sandeep Kumar, Redouane Douali

- HAT_{*n*} compounds render the hole mobility of the order of 10^{-2} to 10^{-4} cm²/Vs.
- The hole mobility decreases with increasing alkyl chain length (*n*).
- Dielectric permittivity at Iso-Col phase transition decreases exponentially with *n*.
- The change in entropy is analogous to the molecular ordering in the columnar phase.